On sampling methods for recovering a clamped cavity in a thin plate

SCAM/CCAM Lunch Seminar

General Ozochiawaeze
Advisors: Isaac Harris and Peijun Li

Department of Mathematics
Purdue University
Email: oozochia@purdue.edu

February 7, 2025

Overview

The Inverse Problem / Motivation

- Send a wave and observe the reflected wave by an unknown obstacle
- **Question:** What information about the obstacle can one extract from the observed wave?
- **Type of waves:** *flexural waves observed in thin elastic plate bending* (modelled by the biharmonic wave equation)
- **Applications:** nondestructive testing and designing devices for remote sensing, energy harvesting, and vibration isolation via acoustic black hole (ABHs).

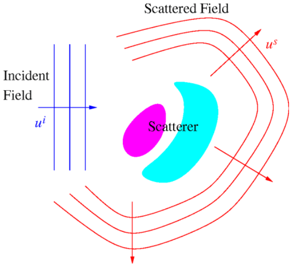

Examples of Applications

infrastructure imaging, elastic cloaking, vibration (noise) control, non-destructive testing,...

Figure: Chladni Plates

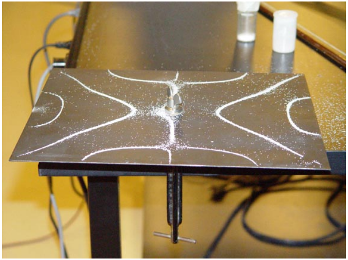

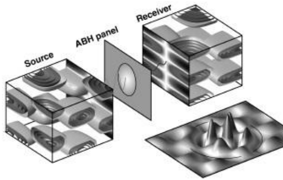

Vibration noise control via Acoustic Black Hole Design

Clamped plates (objects with edges fixed or "clamped" in place) are often used in experiments where vibrations are measured using TV holography for nondestructive testing. Accumulation of sand at nodes of vibrating plate reveals resonance patterns (Chladni Plates)

Acoustic black holes reduce structural vibration and sound pressure control (civil transportation, underwater vehicles, energy harvesting)

Sampling Methods

Examples of sampling methods. *Linear Sampling Method* (Colton-Kirsch, 1996), *Factorization Method* (Kirsch 1998), *Probe Method* (Potthast, 2001), *Reciprocity Gap Method* (Colton-Haddar, 2005),...)

Principle: the idea is to construct an indicator test function $\mathcal{I}(z)$ that will test whether a sampling point z is in the interior or exterior of the scatterer.

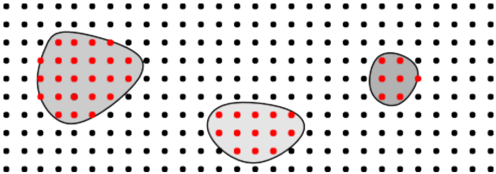

(+) Non-iterative, the computation of $\mathcal{I}$ does not require a forward solver.
(-) Requires a large amount of multi-static data (many transmitters-receivers).

Biharmonic Wave Model

1. $D \subset \mathbb{R}^2$ is a clamped (fixed) cavity with $\partial D \in C^\infty(\mathbb{R}^2)$ and connected complement $\mathbb{R}^2 \setminus \overline{D}$
2. The cavity receives illumination from the incident plane wave $u^i(x) = e^{i\kappa x \cdot d}$
3. The out-of-displacement governed by classical Kirchhoff-Love Model in the purely bending case

The total field $u = u^i + u^s \in H^2_{loc}(\mathbb{R}^2)$ satisfies, with $r = |x|$:

The Biharmonic wave equation

$$\Delta^2 u - \kappa^4 u = 0 \quad \text{in } \mathbb{R}^2 \setminus \overline{D},$$

Clamped boundary Conditions

$$u = 0, \quad \partial_\nu u = 0 \quad \text{on } \partial D,$$

The Sommerfield radiation conditions ($u^s, \Delta u^s$ are outgoing towards infinity)

$$\lim_{r \to \infty} \sqrt{r}\,(\partial_r u^s - i\kappa u^s) = 0, \quad \lim_{r \to \infty} \sqrt{r}\,(\partial_r \Delta u^s - i\kappa \Delta u^s) = 0.$$

DSP. Determine the scattered field u^s from the given bounded domain $D \subset \mathbb{R}^2$ and the differential equation that governs the wave motion.

Biharmonic Wave Decomposition

Introduce the following two auxiliary functions:

$$u_H^s = -\frac{1}{2\kappa^2}(\Delta u^s - \kappa^2 u^s), \quad u_M^s = \frac{1}{2\kappa^2}(\Delta u^s + \kappa^2 u^s)$$

u_H^s is the **Helmholtz component** of u^s and u_M^s is the **modified/anti-Helmholtz component** of u^s such that

$$u^s = u_H^s + u_M^s, \quad \Delta u^s = \kappa^2(u_M^s - u_H^s)$$

u_H^s and u_M^s satisfy the Helmholtz equation and anti-Helmholtz equation respectively. Due to the factorization of the biharmonic wave operator

$$\Delta^2 u^s - \kappa^4 u^s = (\Delta - \kappa^2)(\Delta + \kappa^2)u^s = (\Delta + \kappa^2)(\Delta - \kappa^2)u^s,$$

we obtain

$$\Delta u_H^s + \kappa^2 u_H^s = 0, \quad \Delta u_M^s - \kappa^2 u_M^s = 0 \quad \text{in } \mathbb{R}^2 \setminus \overline{D}.$$

Coupled Scattering Problem

We can reformulate the (DSP) as a coupled system with coupled boundary conditions as follows:

$$\begin{cases} \Delta u_H^s + \kappa^2 u_H^s = 0, \quad \Delta u_M^s - \kappa^2 u_M^s = 0 \quad \text{in } \mathbb{R}^2 \setminus \overline{D}, \\ u_H^s + u_M^s = -u^i, \quad \partial_\nu u_H^s + \partial_\nu u_M^s = -\partial_\nu u^i \quad \text{on } \partial D, \\ \lim\limits_{r\to\infty} \sqrt{r}\,(\partial_r u_H^s - i\kappa u_H^s) = 0, \quad \lim\limits_{r\to\infty} \sqrt{r}\,(\partial_r u_M^s - i\kappa u_M^s) = 0, \quad r = |x|. \end{cases} \tag{1}$$

This decomposition has two advantages:

1. We now have a second-order system instead of a fourth-order problem.
2. The anti-Helmholtz part of the scattered field u_M^s has nice asymptotic behavior when $r \to \infty$. It has exponential decay! (also called 'evanescent component' in literature)

Asymptotic behaviors as $r \to \infty$ are

$$|u_H^s| = \mathcal{O}\left(\frac{1}{\sqrt{r}}\right), \quad |u_M^s| = \mathcal{O}\left(\frac{e^{-\kappa r}}{\sqrt{r}}\right).$$

This is a consequence of their respective Fourier-Hankel series expansions and Bessel function asymptotics.

Well-posedness of Biharmonic Clamped Cavity Scattering Problem

The well-posedness of the biharmonic clamped cavity scattering problem (DSP) has been well studied:

- Variational Method & Riesz-Fredholm theory
  Bourgeouis, L. and Hazard, C. (2020), On Well-Posedness of Scattering Problems in a Kirchhoff-Love Infinite Plate, SIAM Journal on Applied Mathematics 80(3), 1546-1556.
- Boundary Integral Equation Method & Riesz-Fredholm Theory
  Li, P. and Dong, H. (2024), A Novel Boundary Integral Formulation for the Biharmonic Wave Scattering Problem, Journal of Scientific Computing 98(42), 1-29.

Inverse Clamped Cavity Scattering Problem

The outgoing scattered field, also known as the radiating solution, satisfies

$$u^s(x) = \frac{e^{i\kappa r}}{\sqrt{r}} u^\infty(\hat{x}) + O\left(\frac{1}{r^{3/2}}\right) \quad \text{as } r = |x| \to \infty, \quad \hat{x} = x/r$$

- $u^\infty : \mathbb{S}^1 \to \mathbb{C}$ defined on the unit circle is called the far-field pattern.
- We define the far-field operator $\mathcal{F} : L^2(\mathbb{S}^1) \to L^2(\mathbb{S}^1)$ by

$$(\mathcal{F}g)(\hat{x}) = \int_{\mathbb{S}^1} u^\infty(\hat{x}, d) g(d)\, ds(d), \quad \hat{x} \in \mathbb{S}^1.$$

- $\mathcal{F}g = u_g^\infty$, where u_g^∞ is the far-field pattern of the scattered field u_g^s with incident wave $v_g(x) := \int_{\mathbb{S}^1} g(d) e^{i\kappa x\cdot d}\, ds(d)$ (Hergotz wave function)
- The operator $\mathcal{F}$ is compact and has infinitely many eigenvalues.

ISP. Given $\mathcal{F}$ for a range of wave numbers κ (so given far-field data $\{u^\infty(\hat{x}, d) : \hat{x}, d \in \mathbb{S}^1\}$), determine the shape and location clamped cavity D in a thin elastic plate.

Far-Field Patterns Coincide / Uniqueness Result

Because of the exponential decay of the evanescent part u_M^s and $\partial_\nu u_M^s$, the far-field pattern contains only information about the Helmholtz component, thus,

$$u^\infty(\hat{x}) = u_H^\infty(\hat{x}),$$

up to a constant depending on κ. By Rellich's lemma and exp. decay of u_M^s, we note the following:

$$\textbf{FACT}.\ u^\infty = 0 \implies u_H^s = 0 \text{ in } \mathbb{R}^2 \setminus \overline{D}.$$

The anti-Helmholtz component u_M^s generally does not vanish outside of D.
ISP. Given: Far-Field data $\{u_H^\infty(\hat{x}, d) : \hat{x}, d \in \mathbb{S}^1\}$. Want: shape and location of the clamped cavity D. (Note: the clamped cavity can be uniquely determined!)

Theorem (P. Li & H. Dong, 2023)

Let D_1 and D_2 be two cavities meeting the clamped boundary conditions, with corresponding far-field patterns u_1^∞ and u_2^∞ satisfying

$$u_1^\infty(\hat{x}, d) = u_2^\infty(\hat{x}, d), \quad \forall \hat{x}, d \in \mathbb{S}^1.$$

Then $D_1 = D_2$.

Results on Inverse Shape Problem for Biharmonic Plate Equation

- L. Bourgeouis & A. Recoquillay (2020): recovery of clamped cavities and cavities in a free plate with the linear sampling method with near-field measurements (boundary measurements)
  Disadvantage: uses far more multistatic data, namely scattered field and normal derivative of scattered field for point source and dipole
- Y. Chang & Y. Guo (2023): recovery of clamped cavities in a thin elastic plate with near field measurements via the domain decomposition method (optimization method)
- I. Harris, P. Li, & H. Lee (2024): recovery and resolution analysis of clamped cavities with the direct sampling method
- A. Karageorghis & D. Lesnic (2024): method of fundamental solutions (iterative method) for recovering clamped and free plate cavities with near field measurements

Idea Behind Linear Sampling Method

Qualitative/Sampling Scheme
Goal: want to

- recover shape and location of the cavity using an indicator function based on an integral equation solution

Sampling: Collect the far-field data u^∞ and solve an ill-posed linear integral equation for each sample point z

Principle of the Linear Sampling Method (LSM): Characterize the cavity D using the range of the far field operator.

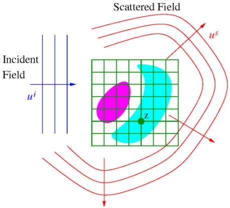

Principle of LSM - The Far-Field Equation

Far-Field Equation.

$$\mathcal{F}g_z(\hat{x}) = \phi_z(\hat{x}), \quad \phi_z(\hat{x}) = -\frac{1}{2\kappa^2}\frac{e^{i\pi/4}}{\sqrt{8\pi\kappa}}e^{-i\kappa x\cdot z}, \quad z \in \mathbb{R}^2,\, g_z \in L^2(\mathbb{S}^1)$$

- $\phi_z(\hat{x})$. far-field pattern of the point source $\Phi(\cdot, z)$ centered at sampling point z
- $\Phi(\cdot, z)$ satisfies $(\Delta^2 - \kappa^4)\Phi(\cdot, z) = (\Delta - \kappa^2)(\Delta + \kappa^2)\Phi(\cdot, z) = -\delta(\cdot - z)$ in $\mathbb{R}^2$ with

$$\Phi(x, z) = \frac{i}{8\kappa^2}\left(H_0^1(\kappa|x-z|) + \frac{2i}{\pi}K_0(\kappa|x-z|)\right), \quad x \neq z$$

  where $H_0^{(1)}$ and K_0 are the Hankel functions of the first kind and MacDonald's function, respectively.

- $\mathcal{F}$ is a compact operator, so the far-field equation is **ill-posed**. In general, a solution g_z does not exist.

  $\Rightarrow$ we can regularize the equation to find an approximate solution g_z^α. The asymptotic behavior of its energy norm will indicate which points $z \in D$.

Approximate Solvability Condition of Far-Field Equation

Want an **approximate solvability condition** for the far-field equation:

Problem

Approximate Solvability Condition: *want to show $\mathcal{F}$ has dense range in $L^2(\mathbb{S}^1)$; that is,*

$$\overline{\textit{Range } \mathcal{F}}^{||\cdot||_{L^2(\mathbb{S}^1)}} = L^2(\mathbb{S}^1)$$

By Hahn-Banach Theorem, this is equivalent to showing the adjoint operator $\mathcal{F}^*$ is injective. By a result called the **reciprocity relation**, the approximate solvability condition reduces to showing $\mathcal{F}$ is injective.

Lemma (Reciprocity Relation)

$u^\infty(\hat{x}, d) = u^\infty(-d, -\hat{x})$ *for every* $\hat{x}, d \in \mathbb{S}^1$.

Why is this useful? This relation can be used to show $\mathcal{F}^* g = \overline{R\mathcal{F}R\overline{g}}$ where $(Rf)(\hat{x}) := f(-\hat{x})$. **Only Need**: $\mathcal{F}$ is injective for approximate solvability.

Helpful Auxiliary Operators to Prove Injectivity

Herglotz wave operator:

$$\mathcal{H} : L^2(\mathbb{S}^1) \to H^{3/2}(\partial D) \times H^{1/2}(\partial D)$$

$$\mathcal{H}g = (v_g, \partial_\nu v_g)^\top \Big|_{\partial D}, \quad v_g(x) = \int_{\mathbb{S}^1} e^{i\kappa x\cdot d} g(d)\, ds(d)$$

Linearity of the map: $u^i \mapsto u^\infty$

$\Rightarrow \mathcal{F}g$ is the far-field associated with the incident field v_g

Therefore: $\mathcal{F}g = \mathcal{G}(-\mathcal{H}g)$

Where $\mathcal{G} : H^{3/2}(\partial D) \times H^{1/2}(\partial D) \to L^2(\mathbb{S}^1)$ is the **data-to-pattern operator**

$$\mathcal{G}(h_1, h_2)^\top := w^\infty, \quad w^\infty = \text{ far field pattern of } w$$

$$\begin{cases} \Delta^2 w - \kappa^4 w = 0 \quad \text{in } \mathbb{R}^2 \setminus \overline{D}, \\ w|_{\partial D} = h_1, \quad \partial_\nu w|_{\partial D} = h_2, \\ \lim\limits_{r=|x|\to\infty} \sqrt{r}\,(\partial_r w - i\kappa w) = 0, \lim\limits_{r=|x|\to\infty} \sqrt{r}\,(\partial_r \Delta w - i\kappa \Delta w) = 0 \end{cases}$$

On Auxiliary Operator $\mathcal{G}$

$\mathcal{G}(h_1, h_2)^\top := w^\infty$

1. w^∞ = far-field pattern of the unique radiating solution $w \in H^2_{\text{loc}}(\mathbb{R}^2 \setminus \overline{D})$ satisfying

$$\begin{cases} \Delta^2 w - \kappa^4 w = 0 \quad \text{in } \mathbb{R}^2 \setminus \overline{D}, \\ w|_{\partial D} = h_1, \quad \partial_\nu w|_{\partial D} = h_2, \\ \lim\limits_{r=|x|\to\infty} \sqrt{r}\,(\partial_r w - i\kappa w) = 0, \lim\limits_{r=|x|\to\infty} \sqrt{r}\,(\partial_r \Delta w - i\kappa \Delta w) = 0 \end{cases}$$

2. To show $\mathcal{G}$ is injective, we need to assume that $\kappa^2 \neq$ eigenvalue of the homogeneous transmission problem (HTP) given by the pair $(p, q) = (w_M, u^i)$ satisfying

$$\begin{cases} \Delta p - \kappa^2 p = 0 \quad \text{in } \mathbb{R}^2 \setminus \overline{D}, \quad \Delta q + \kappa^2 q = 0 \quad \text{in } D, \\ p = q, \quad \partial_\nu p = \partial_\nu q \quad \text{on } \partial D, \\ \lim\limits_{r=|x|\to\infty} \sqrt{r}\,(\partial_r p - i\kappa p) = 0, \end{cases} \tag{2}$$

Approximate Solvability of the Far-Field equation

Lemma.

1. The auxiliary operator $\mathcal{G}$ is compact with a dense range in $L^2(\mathbb{S}^1)$. Moreover, if $\kappa^2 \neq$ an eigenvalue of the (HTP), then $\mathcal{G}$ is injective.
2. We have the following range characterization of the clamped cavity D:

$$z \in D \iff \phi_z(\hat{x}) \in \text{Range}(\mathcal{G}).$$

3. $\mathcal{H}$ is compact and injective.
4. If $\kappa^2 \neq$ eigenvalue of the (HTP), then by superposition $\mathcal{F}$ is injective. Thus, $\mathcal{F}$ has dense range in $L^2(\mathbb{S}^1)$.

The main takeaway. By omitting certain eigenvalues of $\mathcal{F}$, we can approximately solve (using regularization) the far-field equation for g_z. We can characterize the cavity D by using the asymptotic behavior of the solution g_z for different sampling points z.

Theoretical Justification of LSM

Main Theorem. Assume $\kappa^2 \neq$ eigenvalue of the (HTP).

1. Suppose $z \in D$. Given $\epsilon > 0$ there exists an approximate solution $g_z^\alpha \in L^2(\mathbb{S}^1)$ to the far-field equation such that

$$||\mathcal{F}g_z^\alpha - \phi_z||_{L^2(\mathbb{S}^1)} < \epsilon.$$

   Furthermore, $||g_z^\alpha||_{L^2(\mathbb{S}^1)}$ is **unbounded** as $z \to \partial D$.

2. Suppose $z \notin D$. Then for any $g_z^\alpha \in L^2(\mathbb{S}^1)$ such that

$$\lim_{\alpha \to 0} ||\mathcal{F}g_z^\alpha - \phi_z||_{L^2(\mathbb{S}^1)} = 0,$$

   it holds that

$$\lim_{\alpha \to 0} ||g_z^\alpha||_{L^2(\mathbb{S}^1)} = \infty.$$

Choice of indicator function: $\mathcal{I}(z) = ||g_z||^{-1}_{L^2(\mathbb{S}^1)}$.

- If $z \in D$, we expect $\mathcal{I}(z) > 0$.
- If $z \notin D$, we expect $\mathcal{I}(z) = 0$. As $z \to \partial D$, $\mathcal{I}(z) \to 0$.

Algorithmic Aspects

- A regularization is needed to solve the far-field equation, e.g., we used Tikhonov reg. with $\alpha = 10^{-6}$ in all reconstructions

$$(\alpha I + F_d^* F_d) g_z^\alpha = F_d^* \phi_z$$

- Dimension of discretized matrix is based on the number N of sources/receivers. We selected a 250-by-250 grid for each construction.

  Example: 30 sources/receivers yields a 30-by-30 matrix F_d

- $F_d = [u^\infty(\hat{x}_i, \hat{y}_j)]_{i,j=1}^d$. Discretize so that

$$\hat{x}_i = \hat{y}_j = (\cos\theta_i, \sin\theta_j), \quad \theta_i = 2\pi(i-1)/d,\ i = 1, \ldots, d.$$

  We used Li and Dong's boundary integral equation method to approximate the discretized far-field operator F_d.

- Add noise to test the stability of the LSM

$$F_d^\delta = [F_{i,j}(1 + \delta E_{i,j})]_{i,j=1}^d, \quad ||E||_2 = 1.$$

  $E \in \mathbb{C}^{d \times d}$ is a matrix with random entries, $0 < \delta \ll 1$ relative noise level

Numerical Result: Recovering the Apple-Shaped Cavity

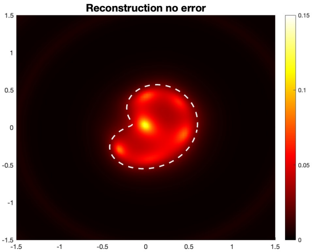

Figure: Recovering the Apple-Shaped Cavity with $\kappa = 2\pi$; no noise; 30 incident and observation directions; 250×250 grid

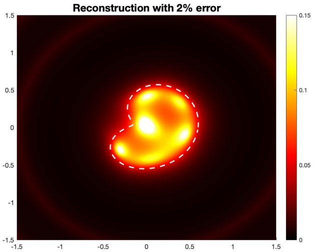

Figure: Recovering the Apple-Shaped Cavity with $\kappa = 2\pi$; noise $\delta = 0.02$; 30 incident and observation directions; 250×250 grid

Parametrization of Apple. $\gamma(t) = \frac{0.55(1+0.9\cos t+0.1\sin 2t}{1+0.75\cos t}(\cos t, \sin t)$

Numerical Result: Recovering the $\partial D \in C^2$ Peach-Shaped Cavity

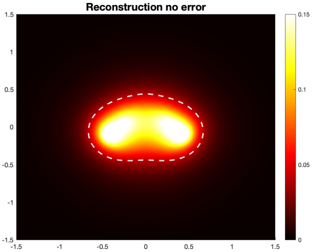

Figure: Recovering the Peach-Shaped Cavity with $\kappa = \pi$; no noise; 30 incident and observation directions; 250×250 grid

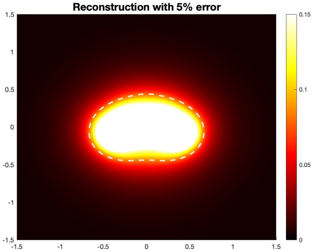

Figure: Recovering the Peach-Shaped Cavity with $\kappa = \pi$; noise $\delta = 0.05$; 30 incident and observation directions; 250×250 grid

Parametrization of Peach. $\gamma(t) = 0.22(\cos^2 t\sqrt{1-\sin t} + 2)(\cos t, \sin t)$

Numerical Result: Recovering the Peanut-Shaped Cavity

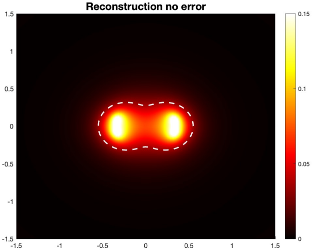

Figure: Recovering the Peanut-Shaped Cavity with $\kappa = \pi$; no noise; 30 incident and observation directions; 250×250 grid

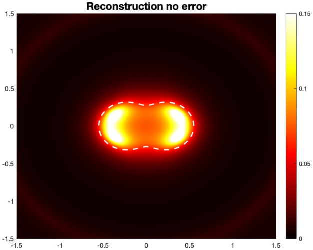

Figure: Recovering the Peanut-Shaped Cavity with $\kappa = 2\pi$; no noise; 30 incident and observation directions; 250×250 grid

Parametrization of Peanut. $\gamma(t) = 0.275\sqrt{3\cos^2 t + 1}(\cos t, \sin t)$

Numerical Result: Recovering the Peanut-Shaped Cavity

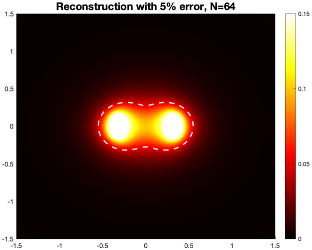

Figure: Recovering the Peanut-Shaped Cavity with $\kappa = \pi$; noise $\delta = 0.05$; 64 incident and observation directions; 250×250 grid

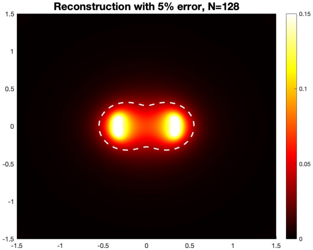

Figure: Recovering the Peanut-Shaped Cavity with $\kappa = \pi$; noise $\delta = 0.05$; 128 incident and observation directions; 250×250 grid

Parametrization of Peanut. $\gamma(t) = 0.275\sqrt{3\cos^2 t + 1}(\cos t, \sin t)$

Conclusion & Future Work

Conclusion:

- Factorization of the far-field operators, showed properties of auxiliary operators important to approx. solvability
- Linear sampling method with far-field measurements for recovering the clamped cavity in a thin plate
- implementation uses lots of multistatic data but less than with near field measurements

Outlook:

- Penetrable media, transmission eigenvalues
- Recovering other cavities (e.g., in free plate, simply-supported plate)
- Single measurement problem: reconstructing partial info on cavities given a single incident plane wave
- Factorization method: what are the necessary criteria for recovery? (LSM only gives sufficient criteria)
- Near-field (boundary measurement) sampling methods